Vol. 2 Issue 1
Jan-April 2021
ISSN 2774-5449

JMEST

Journal of Marine-Earth Science and Technology

itspress

Journal of Marine-Earth Science and Technology
Volume 2 Issue 1. January - April 2021. ISSN. 2774 5499

Editor’s Note :
In the fast-growing of science and technology in marine-earth related topics, we would like to launch a new international journal entitled Marine-Earth Science and Technology Journal (JMEST). The new journal is aimed as a media communication for scientist, researcher and engineer in the field of marine and earth science technology. This journal will receive research and technical papers to be reviewed by our editors and reviewers.
This time, JMEST Vol. 2 Issue 1 consists of 5 papers from Indonesia.

Scopes of Journal :
Marine Science, Naval Architecture, Ship Production Technology, Marine Engineering, Marine Technology, Marine Transportation and Logistics, Ocean Renewable Energy, Earth Science, Physical Oceanography, Ocean and Atmospheric Interaction, Geology and Marine Geology, Geothermal Engineering, Geophysics, Disaster Management and Mitigation, Coastal Environmental Protection.

Table of Contents

MAPPING TSUNAMI HAZARD LEVELS IN PACITAN BEACH USING REMOTE SENSING METHODS

Zahrotin Jamilah, Amien Widodo, Nita Ariyanti
Department of Geophysical Engineering, Institut Teknologi Sepuluh Nopember
email: zahrotinjamilah@gmail.com

ABSTRACT

Pacitan Regency is one of the tourist destinations in East Java with its beauty of tourism from the caves to the beaches that stretch along the southern part of Pacitan. Apart from its tourism potential, Pacitan Regency, which borders the Indian Ocean in the south, has the potential to be hit by a tsunami wave that occurs due to the collision of Eurasian and Indo-Australian plates. By using a remote sensing method, the tsunami hazard level of an area can be seen based on the parameters of the slope, the height of the area, and the distance from the coastline. In addition, the level of exposure of the population is also a factor in determining the level of tsunami hazard. In Pacitan Regency, the area affected by the low level tsunami reached 33753 Hectare, the medium level was 13498 Hectare, and the high level was 3828 Hectare. Areas with a high level of danger are located along the coast which extends in the southern part of Pacitan Regency. The area with the highest level of danger with a wider coverage is around Pacitan Bay. Therefore, it is necessary to have an appropriate mitigation system in reducing the risk of tsunamis, especially around the coast which is used as a tourist destination.

Keywords: Tsunami Disaster, Pacitan Regency, Mitigation, Beach

1. Introduction

Pacitan is one of the cities in Indonesia that provides various natural beauties from cave tours to charming beaches. There are rows of karst hills with caves and underground rivers that extend to the Gunung Sewu Karst area which occurs due to the dissolution of carbonate rocks. There are also a lot of beaches with big waves that stretch along the south of Pacitan Regency, making it as one of the favorite tourist destinations in East Java. This huge tourism potential resulted in high population and the growth of existing buildings around the coast such as hotels. The location of the coast close to the plate collision zone will have a large tsunami potential, so it is necessary to map the tsunami hazard level.

Geographically, Pacitan Regency is located between 110.55^{o}-111.25^{o} East Longitude and 7.55^{o}-8.17^{o} South Latitude. Pacitan has an area of 138.987 hectare which administratively borders Ponorogo Regency in the North, Trenggalek Regency in the East, Wonogiri Regency in the West, and the Indian Ocean in the South. Based on the tectonics that occurred in Indonesia, there are three plates that push each other, namely the Eurasian, Pacific and Indo-Australian plates. Pacitan beach is close to the subduction zone between the plates, namely the Eurasian and Indo-Australian plates, so this subduction will cause an earthquake. An earthquake that occurs on the seabed can trigger a tsunami.

Figure 1. Google Earth Satelite Image of Pacitan Regency

Pacitan Regency has the topography of 85% mountainous and hilly areas, 10% wavy areas, and 5% flat areas. The population is up to 555.30 people, with the highest amount of population in the Pacitan Bay area (BPS, 2020).

Tsunami is one of the disasters that threatens the area around the coast. As a result of the fault that causes an underwater earthquake so that the air will accumulate and be knocked out with high energy. The closer to the land, the higher amplitude of the tsunami waves will be until it reaches several meter, this is because its close location to the plate subduction zone. The tsunami waves that occurred in Pacitan had a height of up to 5.2 m (BMKG, 2019). Areas with a tsunami risk are the urban areas close to the coast, since it has a high level of population and infrastructure development. The level of tsunami hazard in an area can be influenced by the slope, height of the area, distance from the coastline, and population.

The classification levels of the slope class, the height of the area, and distance from the coastline are as in Table 1, Table 2, and Table 3. (Iqbal Faiqoh, 2013)

Score	Slope
5	0-2%
4	3-5%
3	6-15%
2	15-40%
1	>40%

Table 1. Slope Classification

Score	Height Area Classification
5	<10 m
4	11-25 m
3	26-50 m
2	51-100 m
1	>100 m

Table 2. The Height of The Area Classification

Score	Distance from Coastline
5	0-500 m
4	501-1000 m
3	1001-1500 m
2	1501-3000 m
1	>3000 m

Table 3. Distance from Coastline Classification

2. METHODOLOGY

In this study, the tsunami hazard level was determined using remote sensing methods. For the data required for this processing, there are Pacitan Regency administrative data and DEM (Digital Elevation Model) topographic maps which can be obtained from (http://tides.big.go.id/DEMNAS/). The processing method is mapping the slope, the height of the area, and the distance from the coastline based on DEM topographic map data and administrative maps. After that, the scoring of each slope parameter is based on Table 1., the height of the area is based on Table 2., the distance from the coastline is based on

Table 3. The scoring results of each parameter are overlaid and weighted to obtain a tsunami hazard level zone. In this processing using ArcGIS software.

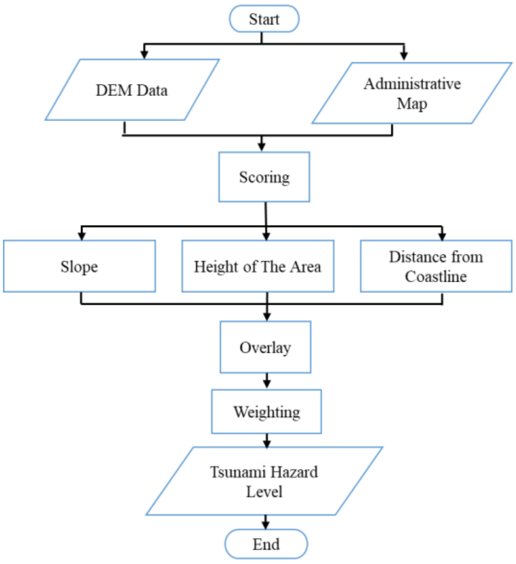

Figure 2. Flowchart

3. RESUTS AND DISCUSSION

The tsunami that occurred in Pacitan Regency was caused by tectonic forces, namely the collision between the Eurasian and Indo-Australian plates. This collision can cause a seabed earthquake with great energy and trigger a tsunami wave that propagates from the epicenter towards the land. Through remote sensing methods, the level of danger from a tsunami can be influenced by several parameters such as slope, height of the area, distance from the coastline, and population.

Figure 3 is a map of the slope class in Pacitan Regency. Based on the slope map, the red color shows the level of the flat slope of 0-2% while the green color shows the slope of the slope is very steep> 40%. In the north, it is dominated by moderate-steep slopes, in the middle it is dominated by steep-very steep slopes, while in the south it is dominated by steep-flat slopes. Steep slopes are located in Punung, Donorejo, Kebon Agung, Tulakan and Sidomoro sub-districts, while medium-flat slopes are in Pacitan, Ngadirojo, and parts of Arjosari districts. Areas with low slope levels and close to the coast will have the potential to be affected by tsunami waves in the event of an earthquake and high waves.

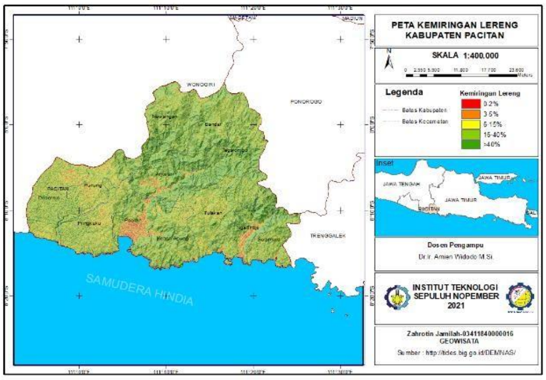

Figure 3. Slope Map in Pacitan Regency

Figure 4 is a map of the altitude class of the region in Pacitan Regency. Based on the map, it is shown that most areas of Pacitan Regency have altitudes ranging from low to very high. For the southern part of Pacitan, most of them have a variation in height of 51-100 meters, while for Pacitan the central part has a height that varies from low to very high, this is because the middle part has a more diverse topography.

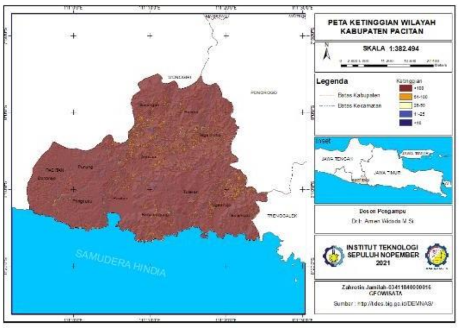

Figure 4. Height Map in Pacitan Regency

Figure 5 is a map of the distance from the coastline. Based on the map, the red color shows the land distance from the near coastline, which is 0-500, the greenish yellow meter shows the distance from the coastline reaching 1501-3000 meters. The distance from the coastline will affect the potential of an area affected by a tsunami wave where the waves propagating to the land will experience a decrease in speed and amplitude as the distance increases so that the farther an area is from the coastline, the potential impact of a tsunami wave will be smaller.

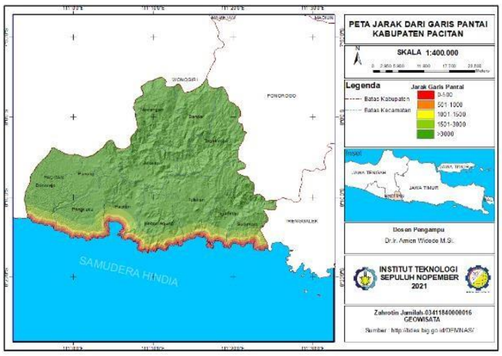

Figure 5. Distance from Coastline in Pacitan Regency

By overlaying and weighting the three parameters, namely the slope, height of the area, and distance from the coastline, the level of tsunami hazard to an area can be seen as in Figure 6. Figure 6 shows the classification of the tsunami hazard level in the Pacitan area starting from low moderate to high. The area affected by the tsunami is shown in Table 4., with a low level reaching 33753 Hectare, a medium level of 13498 Hectare, and a high level of 3828 Hectare. Areas with a high level of danger are areas located on the coast.

Tsunami Hazard Level	Area (Hectare)
Low	33753
Medium	13498
High	3828

Table 4. Tsunami Hazard Level

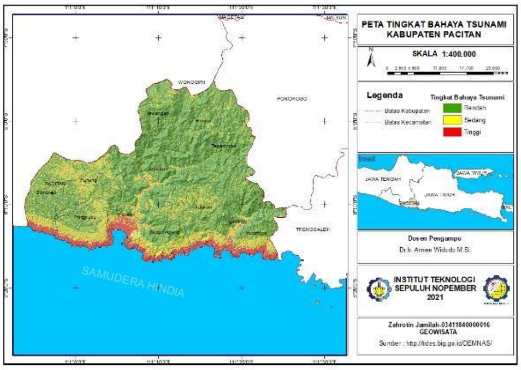

Figure 6. Tsunami Hazard Level Map in Pacitan Regency

As previously explained, the southern part of Pacitan, which is a coastal area, will have a moderate to high tsunami hazard level as indicated by the yellow to red colors. Coastal ranges in southern Pacitan such as Banyu Tibo and Klayar Beaches in Donorejo, Kasap and Srau in Pringkuku, Teleng Ria in Pacitan, and Soge Beach in Ngadirojo will have a moderate-high tsunami hazard because they have a sloping topography with a short distance with the shoreline. In general, the entire southern Pacitan area close to the coastline will have a moderate-high tsunami hazard level. Areas that have a high tsunami hazard level with a wider area are found in Pacitan District, which is in the Pacitan Bay. Tsunami waves that enter the bay area will result in a greater accumulation of energy so that the danger level will be higher. In addition, the level of tsunami hazard can be affected by the level of exposure of the population. Based on Figure 1., the Google Earth Satellite Image map and population data (BPS, 2019), Pacitan District area has the highest population level due to its community activities, settlements, and infrastructure development. Therefore, this area has a higher tsunami hazard level with a wider coverage than the surrounding area.

Based on the map in Figure 6., the southern part of Pacitan coast is an area with a high level of tsunami hazard. Where the beach is a tourist destination that is visited by many tourists, so there is a need for proper mitigation to overcome the risk of a tsunami such as an Early Warning System around the coast, directions and pointers for the nearest evacuation route to reach higher places.

4. CONCLUSION

The level of tsunami hazard can be influenced by several parameters, namely the slope, the height of the area, the distance from the coastline, and the level of exposure of the population. The area of impact in Pacitan Regency with a low level reached 33753 Hectare, a medium level 13498 Hectare, and a high level 3828 Hectare. The high level of danger is in the southern part of Pacitan, especially along the coast and Pacitan Bay. This part of Pacitan Bay has a higher and wider tsunami hazard level because the energy from the tsunami waves will accumulate and become larger, accompanied by low topography and a high infrastructure development.

In the coastal area which is the tourist destination, it is necessary to have an appropriate mitigation effort to deal with the possibility of a tsunami such as the Early Warning System, directions, and evacuation routes for all visitors.

REFERENCES

Anggono, R. S. (2018). PENGURANGAN RISIKO ANCAMAN BENCANA TSUNAMI. 9-13.

BMKG. (2019). Katalog Tsunami Indonesia. 18.

Damayanti, F. H. (2017). APLIKASI SIG UNTUK PEMETAAN ZONA KETERPAPARAN PERMUKIMAN TERHADAP TSUNAMI. *Seminar Nasional Geomatika*, 318-320.

Pacitan, B. P. (2020). Kabupaten Pacitan Dalam Rangka Regency In Figures. 37.

Pacitan, D. K. (n.d.). Potensi dan Produk Unggulan Jawa Timur.

IDENTIFICATION OF LAND COVER CHANGES FROM LANDSAT 8 OLI SATELLITE IMAGERY USING NORMALIZED DIFFERENCE VEGETATION INDEX (NDVI) METHOD (STUDY CASE: SURABAYA)

Syafira Alif Yusroni[1], Vahira Tri Kemalasari[1] and Dhea Pratama Novian Putra [1]
[1] Geophysical Engineering, Institut Teknologi Sepuluh Nopember, Surabaya, Indonesia
email: Syafiraalif28@gmail.com

ABSTRACT

Changes in land use in an urban area, such as Surabaya have a major influence on the balance of nature and the environment of its people. Analysis related to changes in land use from time to time is important to maintain the dynamics of development in Surabaya. The land use identification method in this study utilizes the Normalized Difference Vegetation Index (NDVI) to identify the effect of differences in the spectrum due to vegetation and non-vegetation. Satellite image data is analysed based on the spectrum and the results of the land cover classification have been obtained. From six classes of land cover classification results, it was found that the largest decreasing trend in the area was in class 6, one of which contained urban forest around 13% to 9%. For the trend of increasing area, the largest area occurs in class 5, which includes a land cover of undeveloped land which has the potential for building and infrastructure construction to be carried out around 15% to 19%. Surabaya has a development pattern on the use of vacant land for public and private facilities, which has the potential to reduce the area of an urban forest. Given that the function of forests in urban areas is quite necessary for the stability of air temperature and maintaining the beauty of the city.

Keywords: Land cover, NDVI, Vegetation

1. INTRODUCTION

Urban areas are the main part of the main activities, namely the centralization and distribution of government service activities, social services, economic activities (Dwijayanti and Haryanto, 2015). The use of land in urban areas has increased from year to year with dynamic population growth. This land use requirement must pay attention to the carrying capacity of the scientific function of the land itself. One of the city areas which is the center of government and the capital of East Java (Dirk P. P. Misa et al., 2018). The built area of Surabaya City covers almost 2/3 of the total area. This development is dominated by the construction of residential areas housing) and commercial facilities. The spatial condition of Surabaya has significantly decreased, which indicates that changes in agricultural land, empty land, and green open land / green lines have turned into residential, trade and service areas(Putra et al., 2011). This occurred due to changes in the land cover condition of Surabaya.

Based on The 1945 Constitution of The Republic of Indonesia number 4 at article 12 in 2011, land cover is a line depicting the boundary of the appearance of the area above the earth's surface which consists of natural and/or artificial landscapes (Kementerian Lingkungan Hidup dan Kehutanan, 2015). Information on land cover can be used to model and understand current natural phenomena such as climate change, interrelationships between human activities and global change. This land cover information with maps can be obtained through remote sensing data which provides information on the spatial diversity of the earth's surface. This remote sensing data is an important factor for conducting land cover classification.

This study is aimed to classify land cover using Landsat 8 imagery using the Normalized Difference Vegetation Index (NDVI) method. NDVI is a method that compares the level of vegetation in satellite image data. So that it can be used to analyse the land cover of Surabaya.

2. METHODOLOGY

2.1 Data and Research Areas

The research was conducted in the central part of East Java, Surabaya. The data in this research using secondary data consisting of data Landsat 8 Operational Land Imager (OLI) Satellite Image from 2016 until 2020 and Rupa Bumi Indonesia (RBI) Map. The selection of Landsat 8 OLI Satellite Image was carried out every year in the last five years, in detail on 21st August 2016, 8th August 2017, 24th June 2018, 1st October 2019, and 3rd October 2020. Landsat 8 OLI Satellite Image is secondary data that can be accessed through the USGS (United State Geological Survey) website. And the RBI map can be accessed through Ina-Geoportal Badan Informasi Geospasial (GIS) website and used to cut Landsat 8 OLI Satellite Image with the study area

The data will be used to identify cloud cover. This is done because it can affect the image of the earth's surface recording, so that the research location cannot be seen properly from satellite imagery. Data in 2016 may have inaccurate results because there is little cloud intrusion which can affect the distribution of the colour spectrum in the Normalized Difference Vegetation Index (NDVI) process.

a

b

c

d

e

Fig. 1 Natural landsat 8 OLI satellite image level 1 of Surabaya at (a) 2016; (b) 2017; (c) 2018; (d) 2019; and (e) 2020

2.2 Land Cover Processing

The research is a quantitative study using real data in the form of numbers for the presentation. Identification of land cover is obtained by using the NDVI (Normalized Difference Vegetation Index) extraction method for Landsat 8 OLI Satellite Imagedata each year. The flow chart used is as follows:

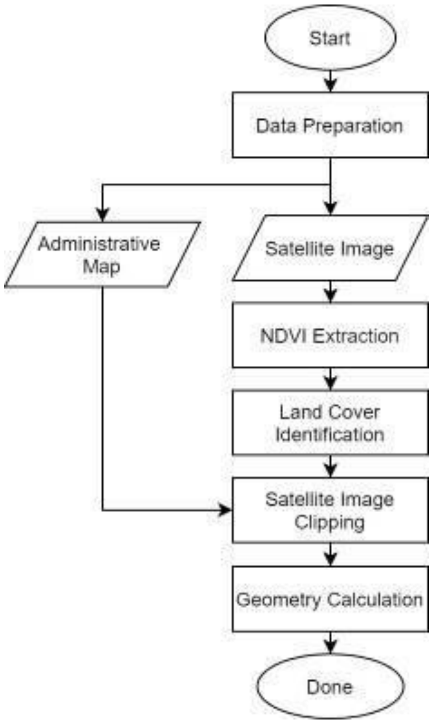

Fig. 2 Research flowchart

NDVI (Normalized Difference Vegetation Index) extraction has a range pixel value of -1 up to 1. Which the vegetation class is in range 0 up to 1, and if a value close to or equal to 1 is a vegetation area with high density. The non-vegetation class is in the range of -1 up to 0. Pixel values that are less than 0 with a range of -0.14 up to 0.3 which is indicated by a dark shade indicate that the object is not classified as a vegetation or non-vegetation class (T. Lillesand et al., 2015). In the extraction process, the NDVI value is obtained by calculating Near Infrared with Red reflected by plants with the equation down below (Sobrino et al., 2008).

$$NDVI = \frac{NIR - Red}{NIR + Red}$$

NIR is the near infrared radiation from the pixels (band 5) and Red is the red-light radiation from the pixels (band 4).

In the NDVI extraction classification, the image can be cleaned up using Enable Smoothing and Enable Aggregation. Enable Smoothing is used to remove specking noise in the image. The numbers used are odd numbers with three as the default value. And Enable Aggregation is used to remove small areas in the image (Harris

Geospatial Solutions, Inc., 2020). After the NDVI extraction classification has been done, the land cover identification uses an approach secondary data by using remote sensing, Google Earth. So, we could find out the real situation in research area. Furthermore, cutting the image is done as an effort to cut the Landsat image so that it fits the research area using an administrative map using the ArcGIS 10 software.

The following are the results of the NDVI classification before processing on ArcGis 10.

Fig. 3 Validation NDVI classification results with satellite imagery from Google Earth

From figure 3 above, the NDVI land cover classification is carried out and percentage in the table below.

Table 1. Land cover classification

Class	NDVI Color	Land Cover
1	Red	Ponds and River estuary
2	Orange	Ponds and Industrial warehouse
3	Yellow	Buildings and A densely populated settlement
4	Light Green	Settlement, Park, and Garden
5	Moss Green	Reeds, Shrubs, and Undeveloped land
6	Dark Green	Urban forest areas, Ponds, and Farmland

3. RESULT AND DISCUSSION

3.1 Results

After processing and classification of NDVI is completed, land cover map are produced as follows.

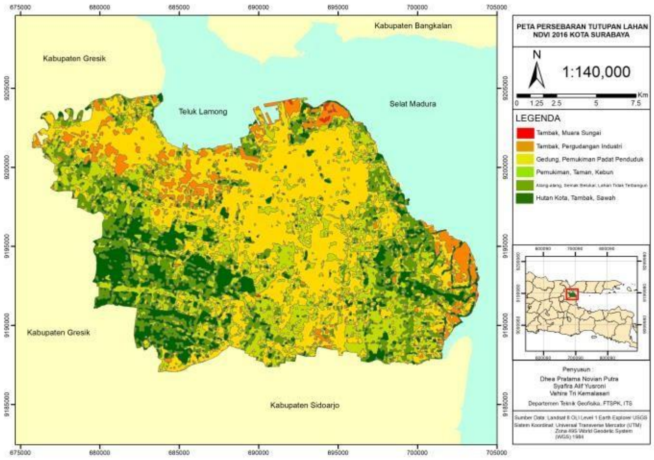

a

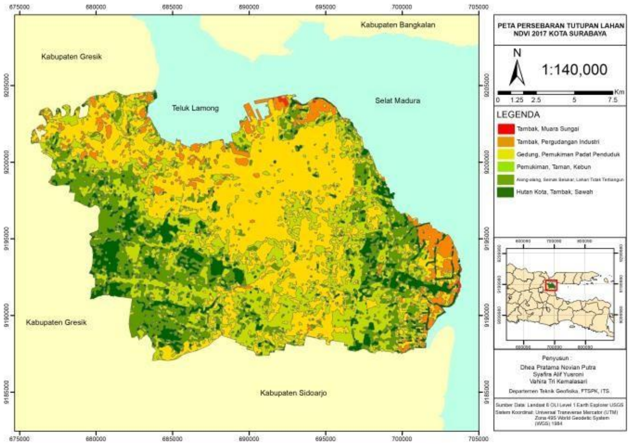

b

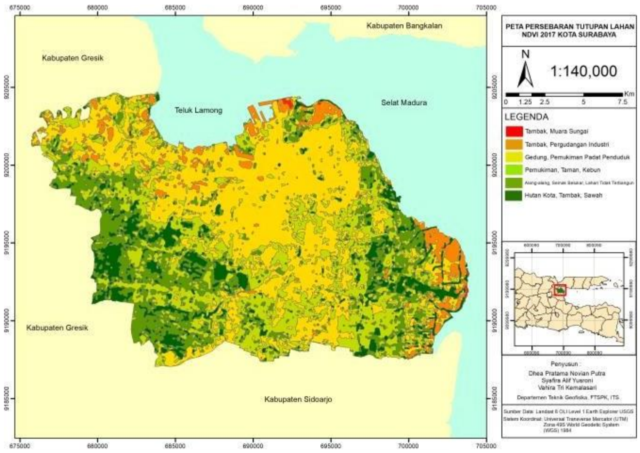

c

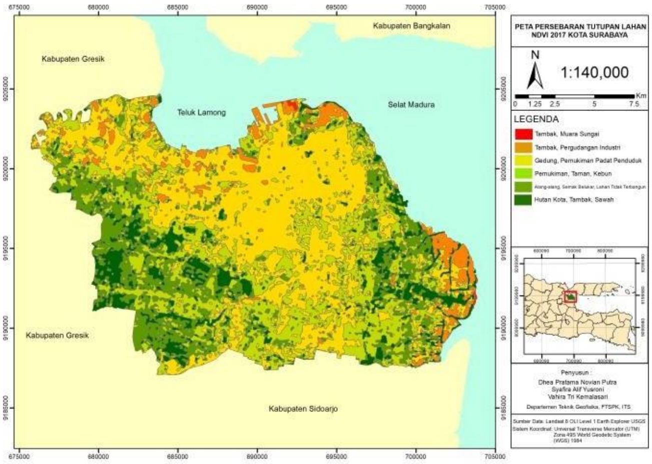

d

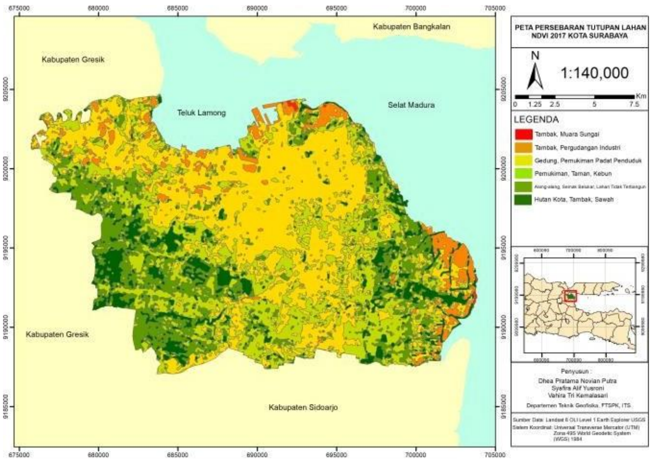

e

Fig. 4 Land cover maps of Surabaya at (a) 2016; (b) 2017; (c) 2018; (d) 2019; (e) 2020

From the land cover map above, it can be identified the pattern of land use change in Kora Surabaya from 2016 to 2020. The dynamic pattern of land use change and its area is presented in the table below.

Table 2. NDVI Land cover area of Surabaya in 2016

Class	Area (ha)	Percentage area (%)
1	69.67367	0.212053404
2	2094.145	6.373576557
3	12834.45	39.06195194
4	8169.804	24.86498436
5	5192.818	15.80446092
6	4495.768	13.68297282

Table 3. NDVI Land cover area of Surabaya in 2017

Class	Area (ha)	Percentage area (%)
1	57.7823	0.175861733
2	1787.554	5.440461556
3	12535.88	38.15323217
4	9126.064	27.77538256
5	6006.186	18.279963
6	3343.198	10.17509898

Table 4. NDVI Land cover area of Surabaya in 2018

Class	Area (ha)	Percentage area (%)
1	126.6271	0.385392425
2	3371.389	10.26090006
3	13543.52	41.22001889
4	6858.375	20.87361968
5	5543.648	16.8722183
6	3413.101	10.38785064

Table 5. NDVI Land cover area of Surabaya in 2019

Class	Area (ha)	Percentage area (%)
1	28.85416	0.08781829
2	886.3564	2.697645877
3	10859.06	33.04978336
4	1138.771	34.66198382
5	7369.54	22.4293616
6	2324.085	7.073407056

Table 6. NDVI Land cover area of Surabaya in 2020

Class	Area (ha)	Percentage area (%)
1	65.26823	0.198645336
2	2327.999	7.085318509
3	13062.28	39.755349
4	7792.84	23.71768718
5	6546.929	19.92572833
6	3061.344	9.317271641

From the data interpretation of land area each year above, it can be modelled in the form of a graph showing the trend of data distribution on each area of land taken each year. The graph of the land distribution in each grouping class is configured as follows:

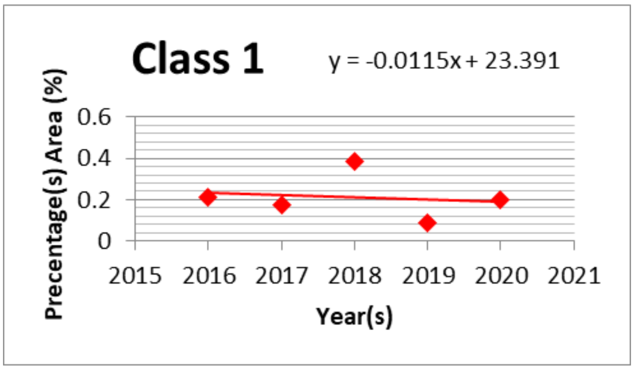

a

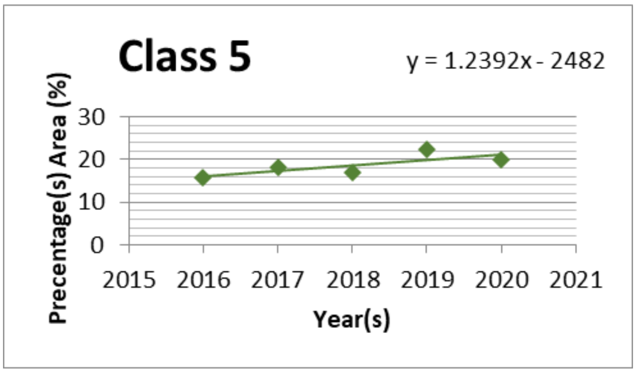

e

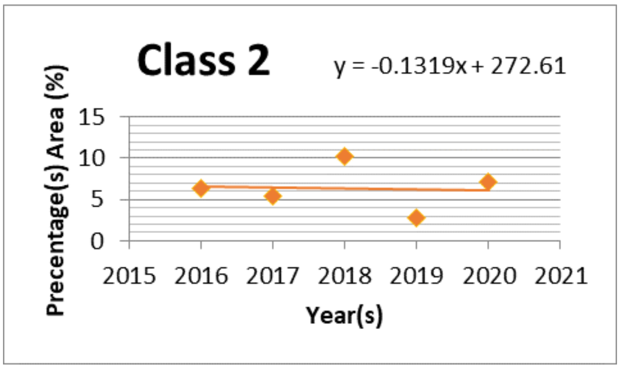

b

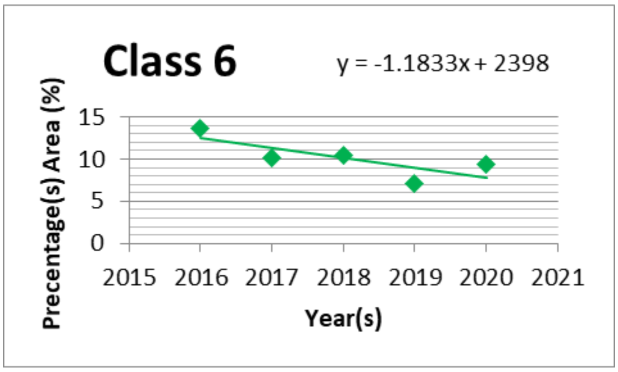

f

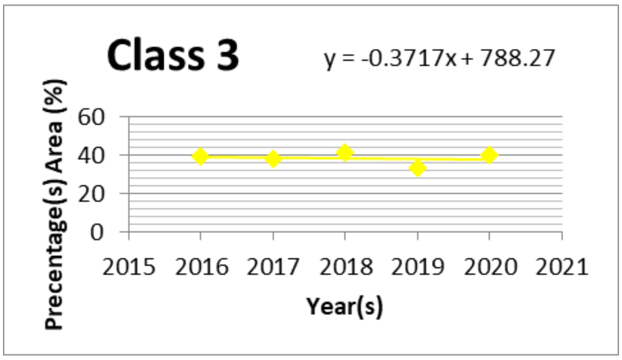

c

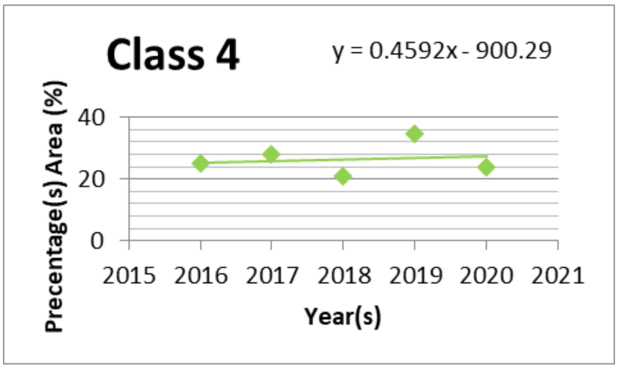

d

Fig. 5 Graph of NDVI land cover trend in Surabaya at (a) class 1; (b) class 2; (c) class 3; (d) class 4; (e) class 5; and (f) class 6

3.2 Discussion

Based on the results of processing and data analysis, it shows the trend of changes in the percentage of dynamic land use in the Surabaya area from 2016 to 2020, where there was an increase in the percentage of land use for class 4 (residential, park, and garden). and class 5 (reeds, shrubs, and undeveloped land) with the largest increasing gradient occurring in class 5. For other classes, there is a tendency to decrease the percentage of land use for class 1 (ponds and river estuaries), class 2 (ponds and industrial warehousing), class 3 (buildings and densely populated residential), and class 6 (urban forest, ponds, farmland), with the largest downward gradient occurring in class 6. The two classes that have opposite gradients (class 5 increase, class 6 decrease) indicate a significant change in land-use changes from urban forest areas, ponds, and farmland to areas of reeds, shrubs, and undeveloped land. Undeveloped land is managed by private or government owned. Most of these class 5 areas are open land that is deliberately allowed to overgrow with wild plants so that some of them become swamps (especially in coastal areas) or land that is under infrastructure or residential construction.

If it is based on the change in the trend of the two classes, it is known that there is a pattern of development movement in the Surabaya towards the use of vacant land to be maximized into facilities for the community as well as for the private sector. This change opens up the potential which will continue to reduce the area of the urban forest into construction areas that are not always accessible for the benefit of the general public. Changes related to reducing urban forest areas also need to be followed up. This refers to the function of the existence of forests in urban areas itself which is quite necessary, where in addition to stabilizing air temperatures and reducing greenhouse gases. Urban forests are also needed in maintaining the beauty of a city and reducing negative impacts from the environment that lead to natural instability in urban areas.

4. CONCLUSION

Based on OLI 8 Landsat image data processing using the NDVI method, it is known that there are dynamic changes in land cover patterns, especially land subsidence in class 6 in the form of forest, ponds, rice fields which can result in air temperature in the area of Surabaya.

REFERENCES

Dirk P. P. Misa, Ingerid L. Moniaga, Verry Lahamendu, 2018. Penggunaan Lahan Kawasan Perkotaan Berdasarkan Fungsi Kawasan (Studi Kasus : Kawasan Perkotaan Kecamatan Airmadidi). Spasial 5, 171–178.

Dwijayanti, A., Haryanto, T., 2015. Evaluasi Tutupan Lahan Permukiman Terhadap Rencana Detil tata Ruang Kota (RDTRK) Surabaya Pada Citra Resolusi Tinggi Dengan Metode Klasifikasi Berbasis Objek (Studi Kasus: UP XI Tambak Osowilangon dan UP XII Sambikerep). GEOID 10, 111–119.

Harris Geospatial Solutions, Inc., 2020. Image Change in Using ENVI. L3HARRIS GEOSPATIAL. URL https://www.l3harrisgeospatial.com/docs/imagechange.html.

Kementerian Lingkungan Hidup dan Kehutanan, 2015. Peta Penutupan Lahan Indonesia. Webgis Kementeri. Lingkung. Hidup Dan Kehutan. URL http://webgis.menlhk.go.id:8080/pl/pl.htm.

Putra, I.N.D.P., Anwar, N., Utomo, C., Sukojo, B.M., Setiawan, N., 2011. Evaluasi Penggunaan Lahan dan Prediksi Perkembangan Sektor Primer , Sekunder dan Tersier Pada Wilayah Kota Surabaya Berdasarkan PDRB. Kern J. Ilm. Tek. Sipil 1, 35–46.

Sobrino, J.A., Jimenez-Munoz, J.C., Soria, G., Romaguera, M., Guanter, L., Moreno, J., Plaza, A., Martinez, P., 2008. Land Surface Emissivity Retrieval From Different VNIR and TIR Sensors. IEEE Trans. Geosci. Remote Sens. 46, 316–327. https://doi.org/10.1109/TGRS.2007.904834

T. Lillesand, R. W. Kiefer, J. Chipman, 2015. Remote Sensing and Image Interpretation, 7th ed.

IMPROVED PROPELLER EFFICIENCY OF A FERRY SHIP WITH ASYMMETRIC PRE-SWIRL STATOR

Andi Haris Muhammad*), Muhammad Iqbal Nikmatullah, Ummi Kalsum A.L.
Department of Marine Engineering, Faculty of Engineering, Hasanuddin University, Gowa 92171, Indonesia.
*e-mail: andi_haris@ft.unhas.ac.id.

ABSTRACT

The International Maritime Organization (IMO) has introduced the importance of the Energy Efficiency Design Index (EEDI) to anticipate global warming and depletion of fuel oil through the development of an Energy Saving Device (ESD) in ship propulsion systems. Pre-swirl stator is a type of ESD installed in front of the propeller which aims to increase propulsion efficiency by reducing the loss of rotational energy in the propeller flow. This study was conducted to determine the effect of 4 blades pre-swirl asymmetric stator diameter on the improved propeller efficiency of KMP Bontoharu using Computational Fluid Dynamics (CFD) software (Ansys-CFX 18.1). The results showed that the use of a pre-swirl stator on the propeller of KMP Bontoharu could increase the propeller efficiency by 6.64% at a stator diameter of 1.1 D_P.

Keywords: Pre-swirl stator; Computational Fluid Dynamic; Propeller efficiency.

1. INTRODUCTION

More than 80% of passenger and cargo transportation is carried out by sea. This marine transportation sector is responsible for more than 30% of CO_2 emissions and around 3 - 4% of CO_2 emissions that have impacted humans (Bennabi et al., 2017). Efforts to reduce the use of fuel oil and exhaust gas emissions (NOx, SOx, and CO_2) in the marine transportation sector as regulated by the International Maritime Organization (IMO) continue to be improved through the development of an Energy Saving Device (ESD) in ship propulsion systems according to the Energy Efficiency Design Index (EEDI) required. The pre-swirl stator is a type of ESD that is installed in front of the propeller. The use of pre-swirl stator has been shown to increase propulsion efficiency by reducing the loss of rotational energy in the flow of the propeller (Takekuma et al., 1981). Some of the advantages of the pre-swirl stator compared to other types of ESD (such as contra-rotating propellers and ducted propellers) are simple shaft system, relatively low cost, high efficiency gains, and high reliability (Kim et al., 2004).

At the beginning, the pre-swirl stator (PSS) design consisted of 6-blades. This type is known as the symmetric axis pre-swirl stator design placed in front of the propeller and has been used on a number of commercial vessels to improve propulsion efficiency of ships. However, the stator design information is not widely found in a number of publications. Takekuma et al. (1981) have conducted some basic research with respect to the pre-swirl stator. They developed the calculation of the Stokes Theorem and simple experiment in designing the pre-swirl stator. The design has been applied to full-scale vessels with an efficiency increase of 7 - 8%. The KRISO Team has developed several fundamental studies about the pre-swirl stator design (Kim et al., 1993 and Lee et al., 1994), particularly related to procedures and analysis of the use of pre-swirl stator (symmetric and asymmetric) in increasing propulsion efficiency through numerical methods and model testing. Kim et al. (2004) have developed a 4-blade asymmetric pre-swirl stator from the previous 6-blade symmetric pre-swirl stator. The pre-swirl stator design configuration with 4-blades which includes 3 stator blades on the starboard and 1 other blade on the port side which called as the starboard stator or vice versa (see Figure 1). They concluded that using a pre-swirl stator with 4-blades on a single propeller increased propulsion efficiency by 5.6% compared to without PSS. Although this result does not increase significantly compared to the use of 6 or 5 blades in previous studies, this reduction of blades can reduce the weight, volume and cost of making the stator by around 30%.

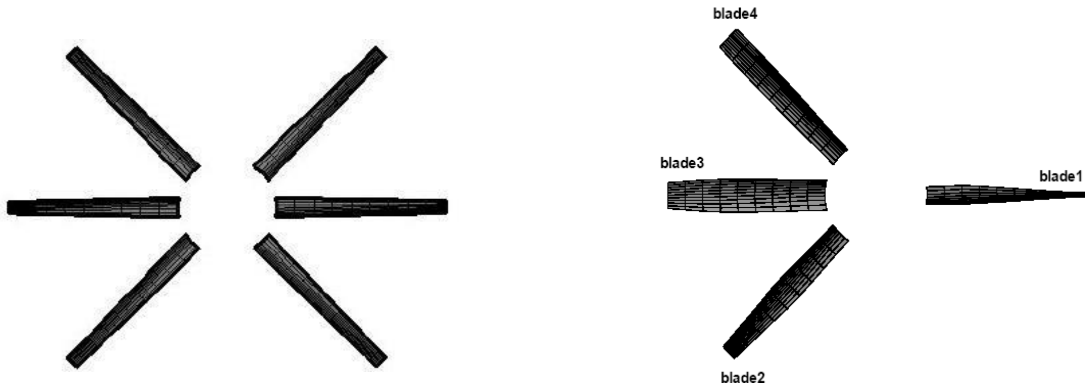

a) 6-blades stator (Takekuma et al., 1981) b) 4-blades stator (Kim et al.,2004)

Figure 1. Blades design of pre-swil stator

Research on the 4-blade asymmetric pre-swirl stator that has been developed by Kim et al. (2004) continued to be improved by a number of researchers through optimization of a number of parameters either through numerical simulations or model testing. Zondervan et al. (2011) and Hassellar and Xing-kaeding et al. (2017) concluded that the usage of pre-swirl stator with a stator diameter greater than the propeller diameter (1.1 D_P) is able to improve propeller efficiency and prevent vortex tip cavitation. While Kim et al. (2013) in their research stated that the effect of this stator diameter has an effect on the amount of torque (Q) on the stator diameter of 1.0 D_P. They also mentioned that the optimum torque is very much influenced by the direction of rotation and the tilt of the stator blades.

Based on the above study, the 4-blades asymmetric pre-swirl stator design has a number of advantages to improve propulsion efficiency and is able to directly reduce fuel consumption and the emission of exhaust gas (NOx, SOx, and CO_2). This paper focuses towards the usage of asymmetric 4-blades pre-swirl stator of improved propeller efficiency of *KMP Bontoharu* ferry ship through CFD Sotware (Ansys CFX 18.1).

2. METHODOLOGY

2.1 Ship Data

KMP Bontoharu has been used as the object of this research. The ship has a capacity of 1050 GT, power propulsion (PB) 2x1000 HP with service speed (V_S) 6,618 m/s is owned by PT (Persero) ASDP Indonesia Ferry and operated on South Sulawesi in Bira-Pamatata crossing route. The lines plan, main dimension and propeller parameters of the ship are shown in Figure 2, Tables 1 and 2, respectively.

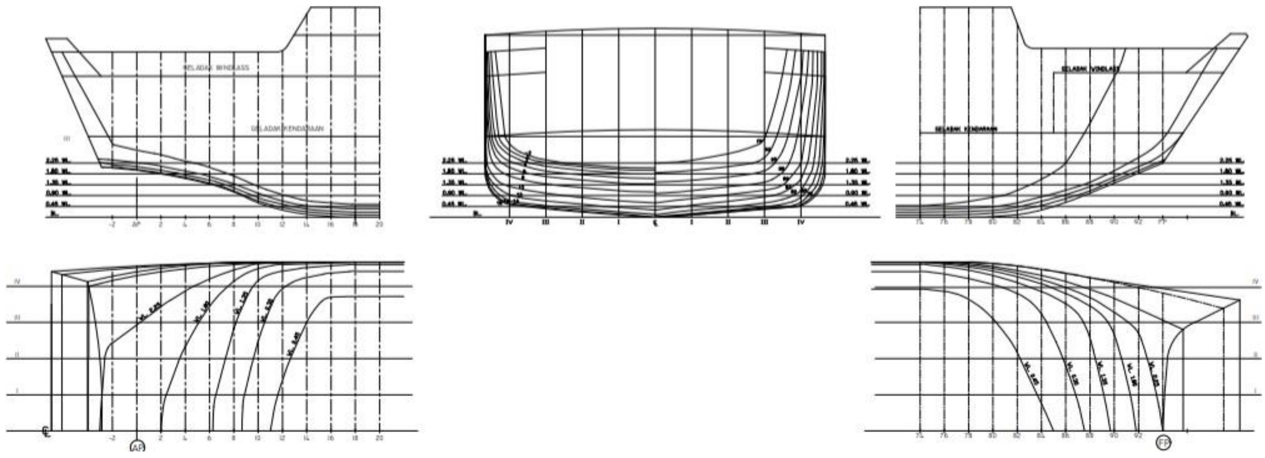

Figure 2. Lines plan of *KMP Bontoharu*

Table 1. Main dimension of ship

Parameters	Dim.
Length between perpendiculars, LBP (m)	47.45
Breadth, B (m)	14.00
Draft, H (m)	2.45
Speed, V_S (m/s)	6.618
Displacement, Δ (ton)	1148

Table 2. Parameters of propeller

Parameters	Dim.
Blade propeller number, Z	2 x 4
Propeller diameter, D (m)	1.422
Blade area ratio, Ae/Ao	0.550
Pitch diameter ratio, P/D	0.928
Propeller revolution, n (rot/s)	8.764

2.2 Design of Pre-Swirl Stator

The design and parameters of the pre-swirl stator (PSS) used in this study are the 4 blades type (Park et al., 2015). The pre-swirl stator is installed 0.5R or 0.335 m in front of the propeller with a distance of 2.3 m between the propellers. The stator blade design and parameters are shown as in Figure 3 and Table 3.

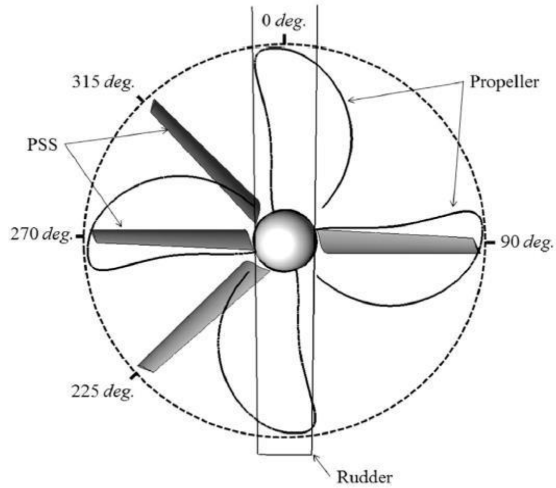

Figure 3. Design of pre-swirl stator blade

Table 3. Parameters of pre-swirl stator blade

Stator	Port side (deg.)	Starboard (deg.)	Angle (deg.)
Blade 1	270	90	7
Blade 2	145	225	10
Blade 3	90	270	8
Blade 4	45	315	4

2.3 CFD Setup

The prediction of thrust force and torque moment affecting the pre-swirl stator in this study uses a commercial CFD software (Ansys-CFX 18.1). The analyzed geometry models including the hull, propeller and pre-swirl stator have been modeled previously with the Rhinoceros 5.0 software as shown in Figure 4. The model of motion fluid flow around the object has been imitated using the incompressible, isothermal Reynolds-Averaged-Navier-Stokes (RANS) equation. This equation was used to determine cartesian flow field and water pressure around the ship model. This equation consists of a general solution of the three-dimensional Navier-Stokes equation, and the Shear Stress Transport (SST) turbulence model has been used in simulation. The SST turbulence model is the best combination model of the two model equations (k-ε and k-ω) (Menter, 2013). The k-ε model is excellent for predicting flows far from the boundary (wall), while the k-ω model is good for flows near walls. Bardina et al. (1997) stated that the SST model is the most accurate turbulent model used for flow modeling in the NASA Technical Memorandum. The turbulent models used by Purnamasari et al. (2017) in CFD simulation to resistance prediction of 17.500 DWT Tanker and compared by experiment. The boundary conditions are formed with a rectangle domain shape as shown in Figure 5. The length, width and height of the domain are 4.5, 3.0 and 3.0 times longer than the ship model (L), as shown by Kim et al. (2017). The dimensions of the domain was made quite long so that the wake shape of the object can be observed and also reducing the wall effect. ANSYS Workbench-CFX-Mesh was used in the meshing process as shown in Figure 6. Then, the element of boundary layer was formed around the object (20 layers) using this mesh. Meanwhile, the tetrahedral (unstructured) mesh is used in the areas that is far from the object.

A grid independence is the number of element to obtain a constant value of propeller thrust. The propeller thrust was compared by the Holtrop method (Holtrop and Mennen, 1982; Holtrop, 1984). Table 4 shows a summary of the propeller thrust from different numbers of elements. It was discovered that by using 3,155,002 elements the error was around -0.01 % and the simulation time 4 hours 20 minutes.

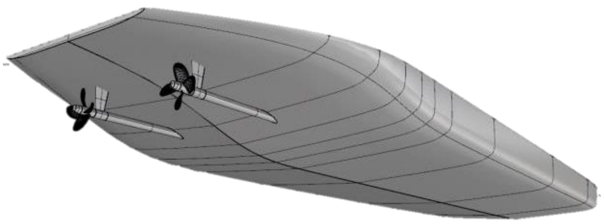

Figure 4. Geometry ship model (hull – propeller - PPS)

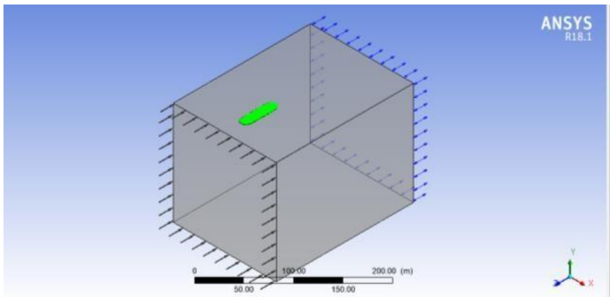

Figure 5. Domain setup

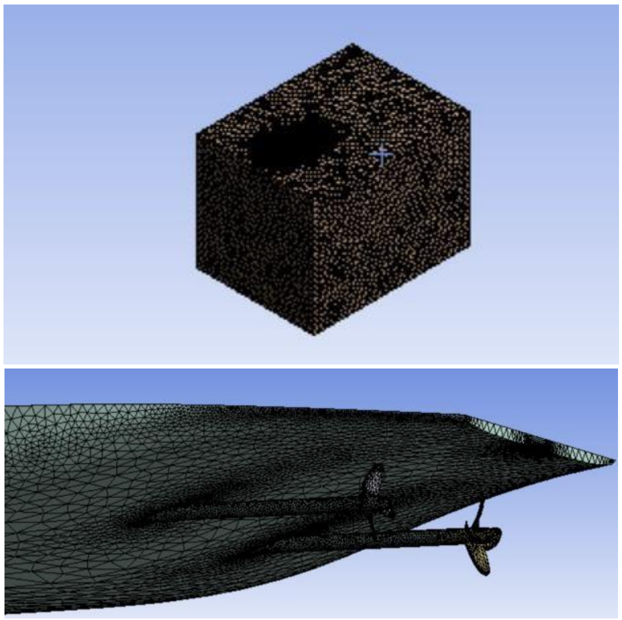

Figure 6. Meshing process

Table 4. Grid independence

Number of Element	867811	1870081	3155002
T	153.736	148.721	143.669
T (prediction)	144.422	144.422	144.422
Percentage (%)	0.06	0.03	-0.01
Time of Simulation	45m	2h 15m	4h 20m

2.4 Data Analysis

The analysis of propeller efficiency (η_P) and propulsive efficiency (η_D) can be predicted by Xing-kaeding et al. (2017) in Equation 1 and 2:

$$\eta_P = \frac{TV_S}{2\pi\, nQ} = \frac{K_T}{K_Q}\frac{J_S}{2\pi} \quad (1)$$

$$\eta_D = \frac{P_E}{P_D} = \frac{R_V V_S}{2\pi\, nQ} = \frac{TV_S}{2\pi\, nQ}\frac{R_T}{T} = \eta_P(1-t) \quad (2)$$

where: T shows the thrust of propeller; Q is the torque of propeller; Vs is the ship speed; n is the propeller rotation; K_T is the thrust coefficient of propeller; K_Q is the torque coefficient of propeller; J_S is the speed advaced coeficient.

3. RESULT AND DISCUSSION

Figure 7 shows the relationship graph between the thrust (kN) and the ship speed (V_S) as a result of the combined hull-propeller model (self-propulsion) simulation with CFD Software (Ansys CFX 18.1). At the ship speed of 6.618 m/s, the thrust is 143.669 kN. This thrust value is 0.42% smaller than the simulation results through the open propeller. However, at a ship speed of 7.618 m/s the value of the thrust is greater than 0.34%. Furthermore, Figure 8 shows the relationship between torque (kN.m) and ship speed (V_S), at speeds of 6.618 and 7.618 m/s, respectively, the torque moment are 21.842 and 22.730 kN.m. The torque value are 9.43 and 9.15% smaller than the simulation results through the open water test. The complete results of the prediction of thrust and torque can be seen in Table 5.

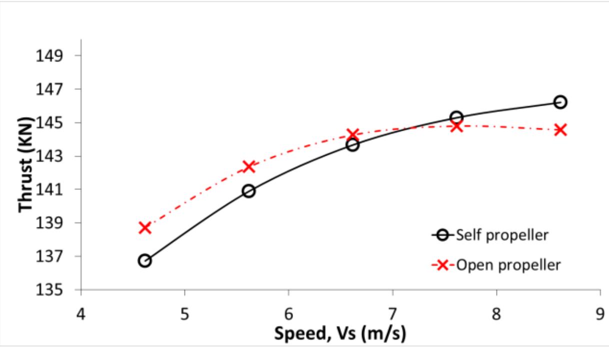

Figure 7. The relationship between thrust (kN) and ship speed (VS).

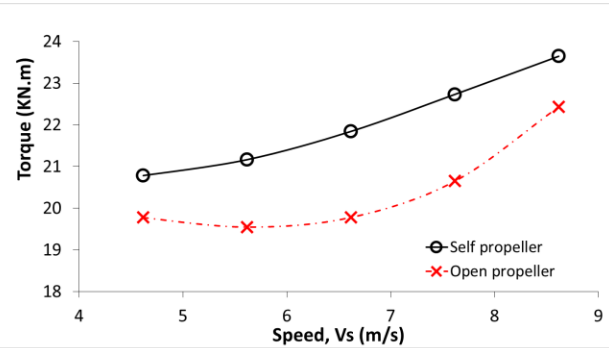

Figure 8. The relationship between torque (kN) and ship speed (V_S).

Figure 9 shows the simulation results of the relationship between thrust (kN) and pre-swirl stator (PSS) diameter (m) at ship speed and propeller rotation constant (Vs = 6,618 m/s and n = 8,764 rot/s) by software CFD software (Ansys CFX 18.1). At the PSS diameter equal to the propeller diameter (D_S = D_P), the thrust propeller is 149,676 kN or 4.18% larger than without the stator. At the same condition, a torque value of 21.96 kN.m is obtained or 0.50% greater than without the stator as shown in Figure 10. Furthermore, Figures 9 and 10 also shows the increasing trend of thrust and torque at D_S = 1.1 and 1.2 D_P.

Figure 11 shows the simulation results of the relationship between propeller efficiency (η_P) and propulsive efficiency (η_D) to changes in the pre-swirl stator diameter (D_S). At the PSS diameter equal to the propelle diameter (D_S = D_P), the propeller efficiency (η_P) and the propulsive efficiency (η_D) were obtained 0.82 and 0.74, respectively. This efficiency value was greater 4.91 and 0.70% than without using stator, respectively. Furthermore, the PSS diameter was greater than the propeller diameter (D_S = 1.1 D_P), the propeller efficiency (η_P) and the propulsive efficiency (η_D) increased by 6.64 and 1.37 respectively compared to without using a stator, while the PSS diameter was greater than the diameter. propeller (D_S = 1.2 D_P) propeller efficiency (η_P) and propulsive efficiency (η_D) were reduced by 5.18 and 0.58%, respectively. The complete results of the propeller performanec prediction are as shown in Table 6. Genaraly, the flow visualisation of the effect of pre-swirl stator's configuration are show in Figure 12 to 17.

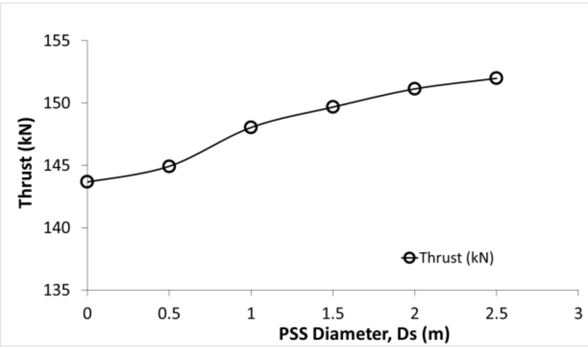

Figure 9. The relationship between thrust (kN) and PSS diameter (m).

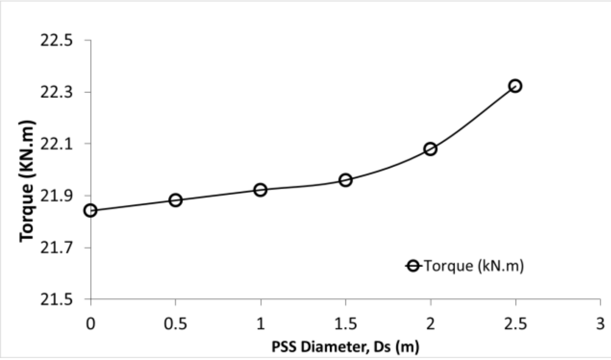

Figure 10. The relationship between torque (kN.m) and PSS diameter (m)

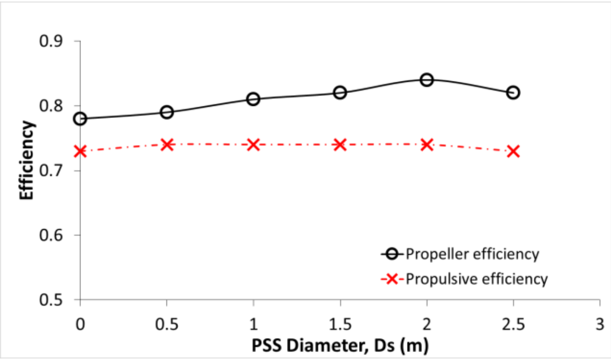

Figure 11. The relationship between propeller efficiency (ηP), propulsive efficiency (ηD) and PSS diameter (DS).

Table 5. Thrust and torque parameter

Speed (m/s)	Thrust (kN)		Torque (kN.m)	
	Self-prop	Open-prop	Self-prop	Open-prop
4.618	136.725	138.718	20.782	19.778
5.618	140.896	142.362	21.164	19.550
6.618	143.669	144.276	21.842	19.782
7.618	145.301	144.810	22.730	20.650
8.618	146.218	144.586	23.644	22.432

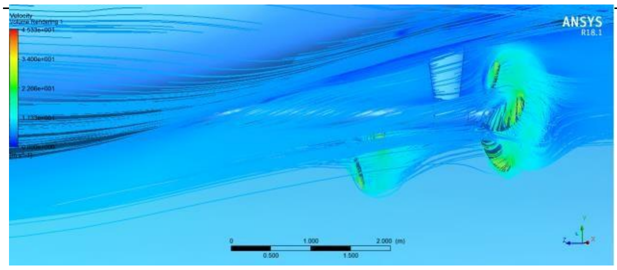

Figure 12. Simulation result without PSS

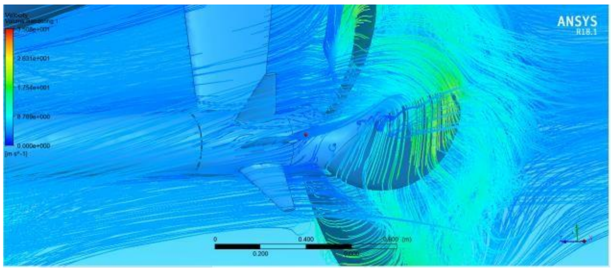

Figure 13. Simulation result with PSS (D_S=0.5 D_P)

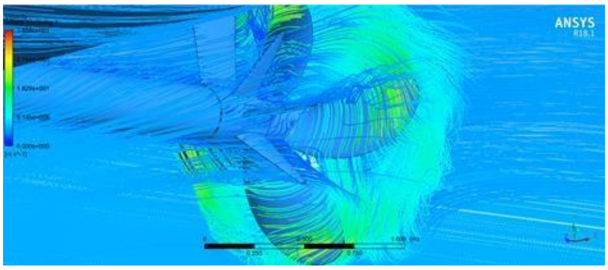

Figure 14. Simulation result with PSS (D_S=0.75 D_P).

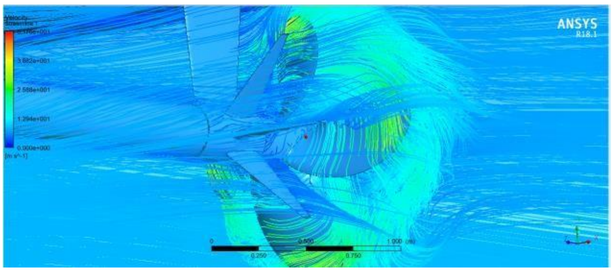

Figure 15. Simulation result with PSS (D_S=D_P).

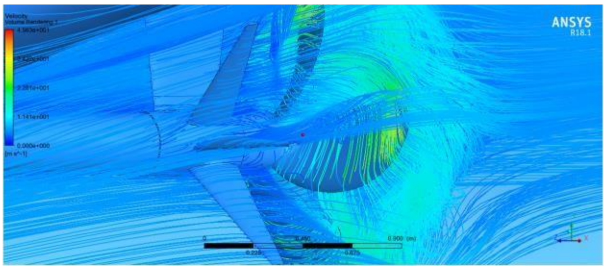

Figure 16. Simulation result with PSS (D_S=1.1 D_P).

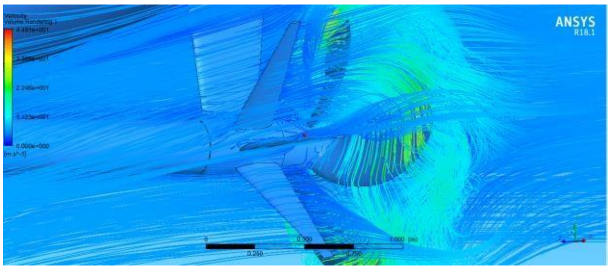

Figure 17. Simulation result with PSS (D_S=1.2 D_P).

Table 6. Propeller performance

Parameters	Stator's Diameter (D_S)					
	wo stator	0.5 D_P	0.75 D_P	1.0 D_P	1.1 D_P	1.2 D_P
n (rot/s)	8.843	8.790	8.773	8.734	8.630	8.703
Vs (m/s)	6.618	6.618	6.618	6.618	6.618	6.618
Thrust (kN)	143.669	144.927	148.038	149.676	151.133	151.982
Torque (kNm)	21.842	21.882	21.922	21.960	22.080	22.322
η_P	0.78	0.79	0.81	0.82	0.84	0.82
ηD	0.73	0.74	0.74	0.74	0.74	0.73
%Gain (ηP)	0.00	1.30	3.49	4.91	6.64	5.18
%Gain (ηD)	0.00	0.42	0.44	0.70	1.37	-0.58

4. CONCLUSION

The pre-swirl stator effect on propulsion system of *KMP Bontaharu* has been analyzed by using CFD software (Ansys CFX 18.1). It was concluded that the use of pre-swirl stator had significantly increased the thrust and torque on the propeller, the increasing thrust and torque is significant with the increase of the pre-swirl stator diameter, while the optimum propeller efficiency is obtained at the pre-swirl stator diameter (D_S = 1.1 D_P) which is equal to 0.84.

REFERENCES

Bardina, J.E., Huang, P.G., and Coakley, T.J. (1997). Turbulence Modelling, Validation, Testing and Development". NASA Technical Memorandum 110446.

Bennabi N, Menana H, Charpentier J.F,, Billard J.Y., Nottelet B. (2017), "Improving Efficiency and Emissions of Small Ships by the Use of Hybrid Electrical Propulsion", *Journal of Power Supply*, Vol. 15, No.2, pp 12-23. DOI:10.13234/j.issn.2095-2805.2017.2.001

Hasselaar, T. W. F. and Xing-kaeding, Y. (2017)," Evaluation of an energy saving device via validation speed /power trials and full scale CFD investigation", *International Shipbuilding Progress*, Vol. 63. No 3-4. pp169–195. doi:10.3233/isp-170127

Holtrop, J. (1984). "A Statistical Re-Analysis of Resistance and Propulsion Data", *International Shipbuilding Progress*, Vol. 31, pp. 272–276

Kim, M.C., Lee, J.T., Suh, J.C. and Kim, H.C. (1993), "A Study on the Asymmetric Preswirl Stator System," *Journal of Society of Naval Architect of Korea*, Vol. 30, No. 1, pp. 30-44.

Kim, M.C. V, Chun, H. H. M. and Kang, Y. D. V. (2004), "Design and Experimental Study on a New Concept of Preswirl Stator as an Efficient Energy-Saving Device for Slow Speed Full Body Ship", *SNAME Annual Meeting* pp. 1–11.

Kim, K., Andersen, M.L., Werner, S. Orych, M., and Choi, Y. (2013), "Hydrodynamic optimization of pre-swirl stator by CFD", *International Shipbuilding Progress*, Vol. 60,No. 1, pp. 233–276. DOI:10.3233/ISP-130092

Kim, M.C., Shin, Y.J., Lee, W.J., Lee, J.H. (2017), "Study on Extrapolation Method for Self-Propulsion Test with Pre-Swirl Device", *Fifth International Symposium on Marine Propulsion smp'17*, Espo, Finland.

Lee, J.T., Kim, M.C., Van, S.H., Kim, K.S. and Kim, H.C. (1994), "Development of a Preswirl Stator System for 300K VLCC", *Journal of Society of Naval Architect of Korea*, Vol. 31, No. 1, pp. 1-13.

Menter, F. R. (2009), "Review of the shear-stress transport turbulence model experience from an industrial perspective", *International Journal of Computational Fluid Dynamics*, Vol. 23, No. 4. pp 305–316. https://doi.org/10.1080/10618560902773387

Park, S., Oh, G., Rhee, S.H, Koo, B.Y., and Lee, H. (2015). "Full scale wake prediction of an energy saving device by using computational fluid dynamics", *Ocean Engineering*, Vol. 101, pp 254–263. doi:10.1016/j.oceaneng.2015.04.005

Purnamasari, D., Utama, I.K.A.P., Suastika, I.K. (2017). CFD Simulations to Calculate the Resistance of A 17.500-DWT Tanker", *The 3rd International Seminar on Science and Technology, Postgraduate Program Institut Teknologi Sepuluh Nopember, Surabaya, Indonesia*. pp 112-116.

Takekuma, K., Tsuda, S., Kawamura, A., and Kawaguchi, N. (1981), "Development of Reaction Fin as a Device for Improvement of Propulsive Performance of High

Block Coefficient Ships", *Journal of the Society of Naval Architects of Japan*, Vol. 150, pp 74–84.

Xing-kaeding, Y., Streckwall, H. and Gatchell, S. (2017), "ESD design and analysis for a validation bulk carrier ", *International Shipbuilding Progress*, Vol. 63, No. 3-4, pp. 137–168. DOI:10.3233/ISP-170126

Zondervan, G., Holtrop, J., Windt, J. and Van Terwisga, T. (2011), "On the Design and Analysis of Pre-Swirl Stators for Single and Twin Screw Ships", *Proceedings of the Second International Symposium on Marine Propulsors - SMP'11.*

OPERATIONAL RISK ASSESSMENT SHIP CONSTRUCTION CAUSES MATERIAL IMPORT USING HOUSE OF RISK (HOR) and CRITICAL CHAIN PROJECT MANAGEMENT: CASE STUDY IN GRESIK SHIPYARD INDUSTRY

Minto Basuki, Oka Hildawan Mahendra
Naval Engineering, Faculty of Mineral and Marine Technology, ITATS
e-mail : mintobasuki@itats.ac.id

ABSTRACT

This research is aimed to conduct risks assessment of ship building process in the part of materials procurement especially imported materials. The problem in Gresik shipyard industry is late material import, which impact the project delay. This research used House of Risk (HOR) combination and Critical Chain Project Management (CCPM) method analysis. Data analysis was obtained from data sample on new construction work of 2 x 1200 HP tug-boat at the Gresik Shipyard. The data used was related with materials procurement especially imported materials. The analysis used House of Risk (HOR) method and obtained 14 risk events which occurred in planning process and imported components for tug-boat 2x1200HP construction and 22 events as risk agent. There were 14 highest risks needing risk mitigation to reduce the impact. Rescheduling result of the material arrival and imported component used Critical Chain Project Management (CCPM) method. It was able to save time duration from activities schedule of 50%; previous schedule was 84 days become 42 days.

Keywords: Imported material; Risk mitigation; Project Management; Risk agent; Risk assessment

1. INTRODUCTION

The shipbuilding industry is an industry with specific characteristics and complex business environment and it is one of industries with high risk and needs careful management (Basuki et al, 2012). Generally, ship builders need such a long time to build a ship in the national shipyard, so they got difficulty to compete with other shipyards. There are four internal strategic factors to the process of shipyard in management, in new shipbuilding activities. Those four internal strategic factors are shipyard management, technology process, product performance (quality and delivery time), and price offer. Meanwhile, there are four strategies for external side, namely interim supply (quality and material specifications), shipbuilding order, global barriers, and policies in maritime sectors. These factors greatly influence the advantage competitive and sustainability of national shipbuilding industrials. The problems had an important effect to the financial risk of shipbuilding companies especially product performance factor and Interim Supply.

In a new shipbuilding process, completing of ship construction of the time agreed in the contract was really important (Cahyani and Pribadi 2016). There are a lot of factors influenced and caused delay of new shipbuilding projects. One of the factors which can delay in ship completing delay is ship materials delay, especially imported materials. Shipyard industry must anticipate the existence of imported materials. It needed an application of risk analysis and risk assessment in order to delay anticipate in project completion (Basuki et al. 2012). It needed to be conducted because risk management analysis and risk assessment in a process of ship building is still few. Because of this reason, it needed risk management analysis related with materials and main components delay. Although shipbuilding process has high risk, risk management application in various cases of shipbuilding production process is still limited (Basuki and Wijaya, 2008; Basuki and Setyoko, 2009; Basuki and Choirunisa, 2012; Basuki et al. 2014).

Basically, qualitative and quantitate risk analysis in risk management is a process of impact assessment and identified risk possibility. This process is carried out by risk arranging based on the impact on project objectives. Basuki and Setyoko (2009), Basuki and Choirunisa (2012), Basuki et al. (2014), Basuki and Putra (2014), Asdi and Basuki (2021) stated that quantitative risk analysis was the numeric probability of analysis process from each risk and its consequence on project objectives. This analysis is usually followed by qualitative analysis and depended on the availability of costs, time, and performance of the company conducting the project.

Critical Chain Project Management (CCPM) is a scheduling project focusing on completing critical chain project in a time and buffer time was the way to change safety time to buffer time. Buffer time consists of feeding buffer and buffer project. Feeding buffer is buffer time connecting non-critical chain activities with critical chain activities. In addition, buffer feeding function is a spare time for delay of non-critical chain activities. Buffer project was a buffer time where was located in the end of critical chain in a project as a spare time to all projects. Both buffer time would ensure critical chain and integrity of project schedule as a whole (Aulady and Orleans, 2016). The research's aim using HOR and CCPM method was to reduce the risk of materials and components delay in a shipbuilding project, so costs, schedules, performances, and qualities are accordance with those sets by the parties involved in the projects.

The process of risk mitigation in materials and main ship components procurement used House of Risk (HOR) method to new shipbuilding project. Risk mitigation was used to rescheduling process by using CCPM method and it allocated in the resources to support accelerate rescheduling, project completing time, reduce costs, and improve company performance.

2. METHODOLOGY

This research was conducted on September to December 2020 on one of shipyards in Gresik. Focusing of this study was assessing the risks delay in materials procurement, especially imported materials in a new shipbuilding project. The research design had several stages; 1) the research objective was the construction of new tug boat 2 x 1200 HP, especially in the materials section, 2) data collection was carried out with primary and secondary data, namely the data from the shipyard, 3) data analysis was conducted with HoR and CCPM methods to determine risk assessment and risk mitigation. Risk analysis stage was used HOR method in phase I. The stage of risk management used HOR in phase II and CCPM method.

3. RESULT AND DISCUSSION

Risk Identification

The result of risk event identification was obtained 14 risk events of materials and import components delay in tug-boat 2 x 1200 Hp construction project as shown in Tables 1 and 2 was the risk agent.

Table 1. Risk Events

Risk Code	Risk Events
Risk Plan of Materials and Components Scheduling Process	
(Unit of Management Project)	
E1	Request error in materials and components purchase
E2	The specification of changing request from the owner
E3	Bad coordination between the units involved
E4	The request schedule changing from the owner
E5	Materials and Components arrival licensing process
The Risk of Materials and Component Procurement Process	
Logistic Unit	
E6	The tardiness of materials and components delivery
E7	Misinformation of materials and components specifications
E8	Incorrect supplier selection
E9	Limited availability of materials and components
E10	Incompatible quantity of materials and

	components
The Risk of Materials and Components Purchasing Process	
Accounting Unit	
E11	Increasing of materials and components price
E12	Lack of funds for materials and components need
E13	Losing of supplier confidence in the company's financial capability
E14	Cost estimating errors in materials and components

Table 2. Risk Agents

Risk Code	**Risk Agent**
Risk Plan of Materials and Components Scheduling Process	
(Unit of Management Project)	
A1	Agreed contract didn't state clearly materials and components type
A2	Unclear and incomplete materials and components data
A3	The supplied doesn't understand data specification of materials and components
A4	Lack of supervision from leadership
A5	Lack of Human resources
A6	Negligent labor (Human Error)
A7	Prioritize more urgent job
A8	Human resources are less competent
A9	There is a pandemic, a natural disaster in the region
The Risk of Materials and Component Procurement Process	
Logistic Unit	
A10	Incorrect supplier selection
A11	The lateness of issuance purchase order (PO)
A12	Materials and components were not available in a supplier
A13	Same spare parts were not available in the market
A14	Administration completion was taking a long time
A15	Long duration of purchase negotiations
A16	Procedure errors
A17	There was no supervision from the supplier
A18	The information data of purchasing order was error
The Risk of Materials and Components Purchasing Process	
Accounting Unit	
A19	Increasing in exchange rate to the Rupiah against foreign currencies
A20	Over budget against the initial budget plan
A21	Bad company track record in supplier payments
A22	Inaccurate budget estimations

Risk analysis with the Aggregate Risk Potential (ARP) value was used as a basic material for mitigating action to the risk agent. Furthermore, the researchers would rank to determine mitigation actions priority on HOR. The result of ARP calculating used severity and occurrence criteria such as Tables 3 and 4.

Table 3. **Criteria of Severity Scale**

Impact			
Score	**Rank**	**Financial**	**Schedule**
5	Very high	The financial loss was more than 300 million Rupiah	Delay was more than 3 months
4	High	The financial loss was around 200-300 million Rupiah	Delay was around 2 to 3 months
3	Medium	The financial loss was around 100-200 million Rupiah	Delay was around 1 to 2 months
2	Low	The financial loss was around 50-100 million Rupiah	Delay was around 0.5 to 1 months

1	Very Low	The financial loss was less than 50 million Rupiah	Delay was less than a half of a month

Table 4**. Criteria of Occurrence Scale**

Score	Possibility	Description	Frequency
5	Almost certainly / often	The event was predicted to happen	The frequency was more than 5 times in a year
4	Most likely / has happened before	The event might happen	The frequency was around 3-5 times in a year
3	Maybe/ able to happen	The event might be happened at some times	The frequency was around 1-2 times in a year
2	Rarely	It could happen but it is not expected	The frequency was not more than a time in 2 years
1	Very rarely	It was happened only in certain situation	The frequency was not more than a time in five years

Mitigation risk from event and agent risks which were measured to the risk rank was presented in Table 5.

Table 5**. Recapitulation of Priorities for Preventive Action Selection**

Rank	PA Code	Preventive Action
1	PA1	Prioritize the planning schedule for materials and imported components purchase compared with other materials purchase
2	PA2	Assign experienced human resources
3	PA8	Provide punishment for workers who did not working according to standard operational
4	PA5	Conducting briefing and coordination with the supplier
5	PA3	Conducting spare budget for materials and imported components in initial budget estimate
6	PA11	Choose suppliers offering cheaper price with good quality
7	PA9	Verify the owner
8	PA14	Make evaluation/ budget monitoring for each month
9	PA12	Improve employees' skills and competencies
10	PA4	Cross subsidies for other budgets
11	PA6	Looking for comparison suppliers who did more professional and competent
12	PA7	Making Standard operational for checking employees' jobs before the leadership checked employees' jobs.
13	PA10	Conduct a survey to several right supplier before the company purchased the materials
14	PA13	Employees displace to another division according to their expertise field

4. CONCLUSION

The result of risk event identifications obtained 14 risk events occurred the process of material planning and imported components on Tug Boat 2 x 1200 HP construction. The result of risk agent identification obtained 22 risk events occurred in a process of materials and imported components planning on Tug Boat 2 x 1200 HP construction. Risk management result used House of Risk (HOR) and it obtained 14 priorities of preventive actions to the risk agent on a process of materials and imported components delay in tug-boat 2 x 1200 HP construction project. The reschedule result of materials and imported components in tug-boat 2 x 1200 HP construction which used Critical Chain Project Management (CCPM) method was reduction amount of the activities schedule duration about 50% from the initial activities schedule. Old schedule was 84 days and new schedule was 42 days after the researchers used CCPM method. To solve reducing schedule problems, the schedule was replaced by additional buffer at the end of each activity. The buffer function was as a buffer time from the end of each activity process. CCPM method could maximize time which have been used as safety time and it could help speed up the process of materials and imported components arrival.

REFERENCES

Asdi, R and Basuki, M., 2021, *Risk Management In Shipbuilding Using Bayesian Network With Noisy-OR*, IOP Conference Series: Materials Science and Engineering.

Aulady, M., dan Orleans, C., 2016, *Perbandingan Durasi Waktu Proyek Konstruksi Antara Metode Critical Path Method (CPM) dengan Metode Critical Chain Project Management (Studi Kasus: Proyek Pembangunan Apartamen Menara Rungkut)*, Jurnal IPTEK Vol. 20, No. 1, ISSN: 1411-7010.

Basuki, M dan Widjaja, S, 2008. *Studi Pengembangan Model Manajemen Risiko Usaha Bangunan Baru Pada Industri Galangan Kapal*, Prosiding Seminar Nasional Teknologi Produksi, Jurusan Teknik Perkapalan, FTMK ITATS.

Basuki, M dan Setyoko, T., 2009, *Risiko Operasional Pada Proses Pembangunan Kapal Fpb 38 Dengan Material Aluminium Di PT. PAL Indonesia*, Prosiding Seminar Nasional Teori dan Aplikasi Teknologi Kelautan (SENTA).

Basuki, M, dan Choirunisa, B., 2012, *Analisa Risiko Proses Pembangunan Kapal Baru 3.500 LTDW White Product Oil Tanker–Pertamina di PT. Dumas Tanjung Perak Surabaya*, Jurnal Neptunus, Volume 18, hal 97-109.

Basuki, M., Manfaat, D., Nugroho, S., and Dinariyana, AAB, 2012, *Improvement of The Process Of New Business Of Ship Building Industry*, Journal of Economics, Business, & Accountancy Ventura, Vol 15, No. 2.

Basuki, M dan Putra, A.A.W., 2014, *Model Probabilistic Risk Assessment Pada Industri Galangan Kapal Sub Klaster Surabaya,* Prosiding Seminar Nasional Aplikasi Sains & Teknologi (SNAST) 2014 ISSN: 1979-911X Yogyakarta,15 November2014.

Basuki, M., Manfaat, D., Nugroho, S., and Dinariyana, AAB, 2014, *Probabilistic Risk Assessment of The Shipyard Industry Using the Bayesian Method*, International Journal of Technology, Vol 5, No. 1, pp 88-97.

Cahyani, Z.D. dan Wahyu Pribadi, W. S.R., 2016, *Studi Implementasi Model House of Risk (HOR) untuk Mitigasi Risiko Keterlambatan Material dan Komponen Impor pada Pembangunan Kapal Baru*. JURNAL TEKNIK ITS Vol. 5, No. 2, ISSN: 2337-3539.

ZONING PRONE TO LANDSLIDES THOUGHT 3D VISUALIZATION USING THE GEO CAMERA APPLICATION IN CIKUYA VILLAGE, CULAMEGA DISTRICT, TASIKMALAYA REGENCY

Siti Nur Aisah[1], Vinki Ari Lesmana[2]

[1] Department of Geography Education, Siliwangi University, Tasikmalaya, Indonesia
[2] Department Geography Education, Siliwangi University, Tasikmalaya, Indonesia
E-mail: sitinuraisyah630@gmail.com

ABSTRACT

Cikuya Village Culamega District Tasikmalaya District, West Java, landslide prone areas that cause material losses and fatalities. The landslide occurred because Cikuya Village is located in the South Mountain Zone with hilly morphology so that it has a steep slope. Other characteristics cause landslides due to high rainfall intensity, geological conditions, soil types, and land use that are not in accordance with the carrying capacity of the environment. Prevention efforts that can be done by measuring the characteristics of landslide prone and 3D visualization zoning maps using map overlays to produce zoning maps and land suitability using ArcGis 10.5 software and Geo Camera applications The results of this study show the characteristics that cause landslides are high rainfall intensity ranging from 2,203 - 3,054 mm / year, Steep slopes range from 8° - 40°, geological conditions (types of rocks) are divided into two types, namely sedimentary rocks and volcanic rocks, podsolic yellow red soil types that are not good in water escape, as well as land use that is not in accordance with the conditions and carrying capacity of the region. The results of the analysis of assessment, weighting and overlay zoning of disaster-prone areas are divided into three "non-prone" hazardous landslide zones with an area of 7,597 hectares, a "prone" zone with an area of 1,972,147 hectares, and a "very vulnerable" landslide vulnerability zone with an area of 256,968 hectares. Further analysis is that land suitability is divided into three "appropriate" zones with an area of 1,057,391 Hectares, "somewhat appropriate" with an area of 1,080,373 Hectares, and "incompatible" with an area of 98,948 Hectares. It is expected that the results of this study can be a reference for the community in recognizing landslide-prone zone areas in Cikuya Village, Culamega Subdistrict, Tasikmalaya Regency.

Keywords: Landslide Disaster, 3D Visualization, Zoning

1. INTRODUCTION

Landslides are the 3rd largest (third) type of disaster in Indonesia after floods and tornadoes. According to the National Disaster Management Agency (BNPB) in 2017 in Indonesia there were 2,862 natural disasters with details of 979 flood disasters, 886 twisters, 848 landslides taking fatalities (DIBI BNPB, 2019). Based on data on the number of residents in Tasikmalaya district in 2018 reached 1,747,318 people. The need for housing will increase to make all land become built regardless of the impact of disasters on an area.

Based on the document of Disaster Management Plan (PRB) Tasikmalaya District 2020-2024 landslide is a disaster with a high level of risk in Tasikmalaya district with a population affected by 471,857 people, exposed land covering an area of 27,535 ha, as well as losses due to landslides reached Rp.1,140,034,000,000 (bpbd Kabupaten Tasikmalaya, 2020). The large number of people affected by landslides is directly proportional to the increasing need for housing so that much land that is not ideal for settlement is forced into a place to lives (Arsyad, 2010). There is a lot of hill trimming, leveling of the slope even the construction carried out on the steep slope or under the slope can destabilize the slope with the threat of great danger (Hakim, Erwin Hilman, 2019).

On 06 November 2018 in Culamega Sub-district there were flash floods and landslides a number of isolated points due to road access covered with avalanche material and caused five deaths (Tribunnews.com, 2017). Cikuya Village District Culamega Tasikmalaya district is a village that is prone to landslides because it is located on a steep slope, if viewed based on the map of disaster insecurity Tasikmalaya. The development of science in the field of Geographic Information Systems facilitates the assessment and visualization of disaster modeling in 3D (Harahap dan Yanuarsyah, 2012). Maps become an important reference for people to understand the condition of residence, but the information made by the government is still too widespread so that the level of error caused will be greater (Eddy Prahasta, 2009). There needs to be a modeling of landslide disaster prone zoning maps that are easier to understand and detail information so that it can be used by various elements of the community and village apparatus as a reference for regional and residential development.

Conditions in the research area are very minimal networks for communication such as constrained internet signals, the unavailability of digital information board screens and the lack of disaster data updates make it difficult for people to understand disaster-prone zoning. Geo Camera application is created to add information about disaster mapping with 3D visualization without the need for internet network. Geo Camera application is considered to be a solution, because people only need to scan barcodes on the map in Cikuya Village so that they can see the map information in 3D and become interactive information.

2. METHODOLOGY

Quantitative descriptive methods are used with data collection techniques through observations, interviews, questionnaires, documentation studies, and literature studies. The population in this study is the entire community of Cikuya Village with a total of 6,353 people or 1,826 households. Sampling techniques used are quota samples by selecting 5 families from 5 hamlets with the worst landslide events from 13 existing hamlets, and purposive sampling for village heads and head of BPBD Tasikmalaya Regency. Data analysis techniques are quantitative analysis, scoring and weighting of each characteristic cause of landslide disasters, as well as map overlays to produce zoning maps and land suitability using ArcGis 10.5 software, Surfer 10, Global Mapper then visualized 3D using geo camera application that has been created.

3. RESULT AND DISCUSSION

3.1 Results

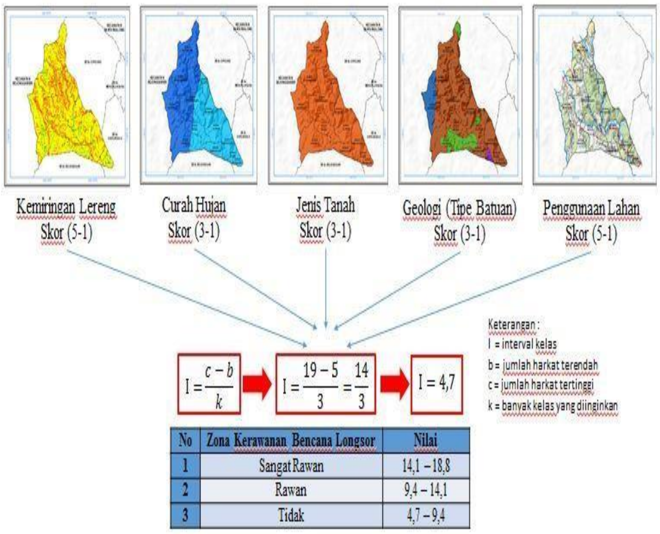

Fig. 1 Overlay landslide-prone zoning of Cikuya Village

The results of the grouping of landslide disaster prone zones in Cikuya Village, Culamega District, Tasikmalaya District are grouped into 3 class intervals in accordance with the calculation of variables, namely the total area between polygon scores and included in the formula according to the research reference. The result of the summation process is then classified based on the classification class of landslide disaster prone to be determined by using the calculation of formulas (Indarto, 2012).

$$I = (c - b) \div k$$

I=(19-5)/3=14/3

I=4.7

Description:

I = class interval

b = lowest number of harkat

c = highest number of harkat

k = many classes

The class interval obtained is 4.7 with a total of 3 classes, so that landslide disaster prone zones are obtained according to the reference of calculated indicators that produce interval values to determine the total value of each interval.

Table 1. Summation of Highs and Lows (2020 Analysis)

No	Variabel	highest score	lowest score
1	Slope	5	1
2	Rainfall Intensity	3	1
3	Geological Conditions	3	1
4	Soil Type	3	1
5	Land Use	5	1

Table 2. Landslide Prone Zone Analysis Results

No	Landslide Prone Zone	Value
1	Very Prone	14,1 – 18,8
2	Prone	9,4 – 14,1
3	Not Prone	4,7 – 9,4

3 categories of zone classification based on interval scoring are:

1) Very prone: the number of scoring >14.1 if the rainfall ranges from 2000 - 3000 mm / year, with a slope of >8 ° (8 ° - 90 °), with the nature of rocks, or berliat-sandy with diverse land use, with an area of 256,968 ha Cikuya Village.

2) Prone: the number of scoring is 9.4-14.1 if the rainfall ranges from 2000 - 3000 mm / year, with slopes ranging from 3 ° - 40 ° , with the properties of rocks with diverse land use, with an area of 1.972,147 Ha Cikuya Village.

3) Not prone: the number of scoring is 4.7-9.4 if the rainfall ranges from <2000 mm /year, with slopes ranging from 0°-3°, with alluvial rock properties or sedimentary with varying land use, with an area of 7,597 ha Cikuya Village.

3.2 Discussion

Cikuya Village located in the southern region of Java Island precisely located at coordinates 7°36'0,764"LS - 108°1'11,672" E or 7,60021222° S – 108.01990889°. The characteristics of landslide-prone areas of Cikuya Village are classified based on scores on 5 aspects, namely slope slope, rainfall, geological conditions, soil type and land use (PVMBG, 2015).

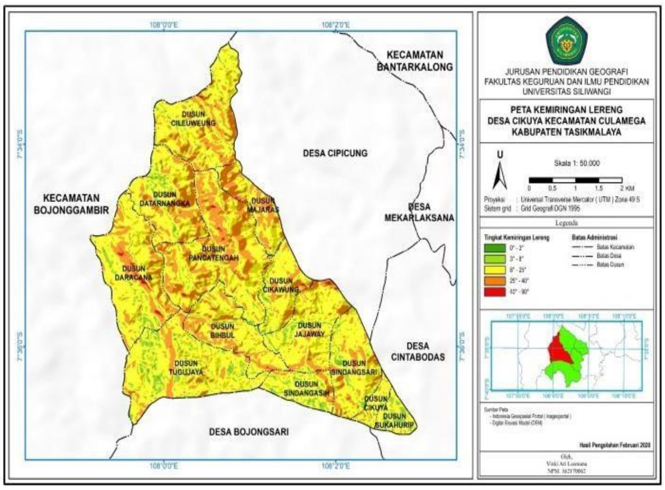

Fig. 2 Slope Map of Cikuya Village

Based on the measurement point in Cikuya Village, Culamega Subdistrict which is divided into 6 measurement points conducted in 5 samples of hamlets that have the worst damage to the purpose to test the slope level against landslide disasters.

No	Lokasi	Lereng				Koordinat
		KL (°)	PL (m)	TL (m)	AL	
1	Titik 1	24,80	70,46	29,53	BD	07°35'43,15"LS - 108°02'50,77"BT
2	Titik 2	20,90	31,89	11,39	TG	07°36'30,95"LS - 108°02'19,49"BT
3	Titik 3	29,90	28,98	14,39	BL	07°35'48,88"LS - 108°01'45,17"BT
4	Titik 4	24,33	18,54	12,44	TML	07°36'03,99"LS - 108°01'17,14"BT
5	Titik 5	29,05	28,27	13,73	TML	07°36'00,70"LS - 108°01'12,14"BT
6	Titik 6	24,09	94,47	23,77	U	07°36'20,03"LS - 108°01'13,01"BT

Fig. 3 Measurement data of cikuya village slope research

Based on the results of slope analysis in Fig. 3 conducted using mapping software get data using Digital Elevation Model (DEM). Slopes with a slope of 8 °-25 ° has the most wide area of 1,483,926 steep categories that have a high risk of landslides that can threaten at any time.

Table 3. Cikuya Village Rainfall Data Scoring

No	Station Name	Rainfall (mm/y)	Score	Area (Ha)	Area (%)
1	Karangnunggal	3.054	3	1.140,563	51%
2	Singaparna	2.203	2	1.096,149	49%
Total				2.236,721	100%

The rainfall data in the table 3 is the highest data for the last five years based on the results of station measurements. Karangnunggal observation station has a high rainfall intensity compared to Singaparna observation station which is 3,054 mm / year with an area of 1,140,563 ha or 51% of the area of Cikuya Village has a score of 3.

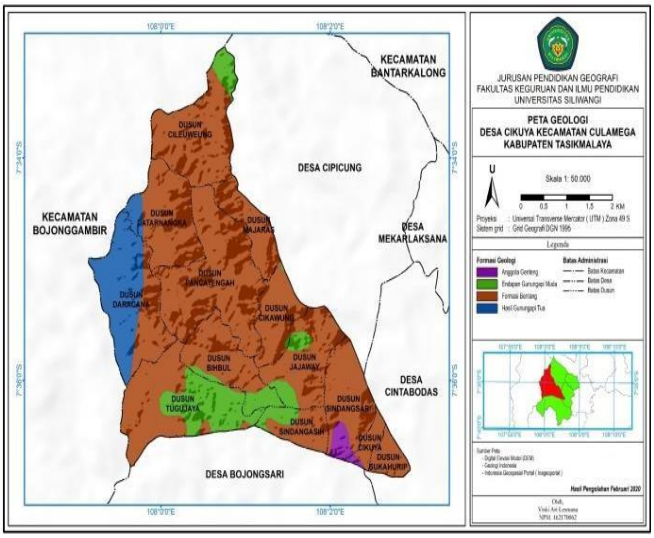

Fig. 4 The geological formations map of Cikuya Village

There are 4 geological formations in Cikuya Village, Culamega District, Tasikmalaya Regency, with the dominance of bentang geological formations at 1,768,712 ha. The effect of landslide disasters due to geological formations or slope builders is less solid sedimentary and volcanic rocks. Weather as a factor that accelerates the occurrence of weathering makes rocks that have rigid properties turn into weathered and easy erosion (Sriyono, 2017).

The land in Cikuya Village varies, with steep slopes, diverse morphology. Land use consists of residential land, rice fields, fields, moors, gardens, forests and shrubs which are the most dominating land. The big problem in Cikuya Village, Culamega Subdistrict, Tasikmalaya, is the lack of understanding of the community about the threat of disasters, especially landslides due to the absence of ancestral heritage regarding landslides.

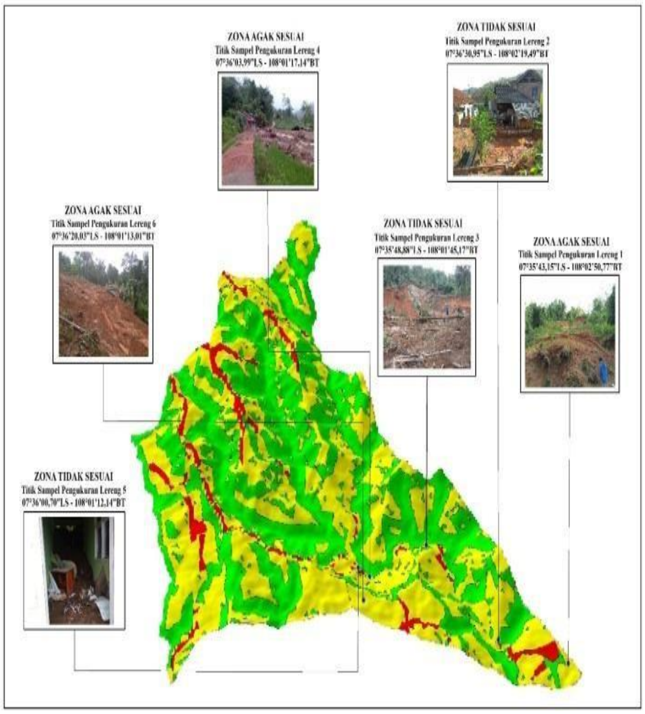

Fig. 5 Type land map of Cikuya Village

Table 4. The result of the calculation of the calculation of land use score of Cikuya Village

No	Land Suitability	Area of the settlement (Ha)	Presentase

1	Appropriate	9,375	16,5%
2	Quite Appropriate	32,823	57,9%
3	Not Appropriate	14,486	25,6%
Total		56,684	100%

Landslide prone zoning through 3D visualization using Geo Camera application in Cikuya Village, Culamega Subdistrict, Tasikmalaya Regency is an analysis process to zone areas that belong to the landslide prone zone. The last 2 years landslide disaster threatens the safety of the community, damages settlements and damages the agricultural area of the community. Landslide material hoarding and closing road access can lead to other disasters such as flooding because the river body is covered with avalanche material. The location of landslide disasters in the last 2 years based on the results of vloting in the field scattered almost all hamlets. Landslide points that occur in the research area are on the use and closure of different land, starting from landslide disasters that occur in the settlement of cikuya village, landslide disasters that occur in agricultural land such as rice fields, plantations, moors and farmland residents, then landslide disasters that occur on steep cliffs filled by shrubs.

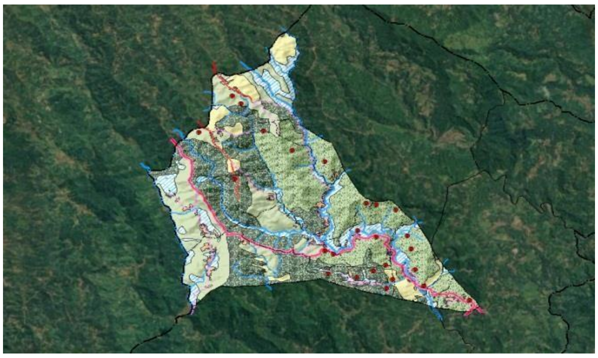

Fig. 6 Landslide points in Cikuya Village

Landslide prone zone in Cikuya Village, Culamega sub-district is divided into 3 insecurity zones and further analysis is carried out which is divided into 3 categories of land suitability. The reference guidelines in determining landslide disaster prone zones and land suitability analysis refer to the reference indicators of Determination of Land Movement Vulnerability Zone by PVMBG (2015), Regulation of the Head of National Disaster Management Agency No. 2 of 2012, Regulation of the Minister of Public Works No. 22 of 2007 concerning Spatial Arrangement of Landslide Prone Areas, and Basic Concepts of Spatial Analysis.

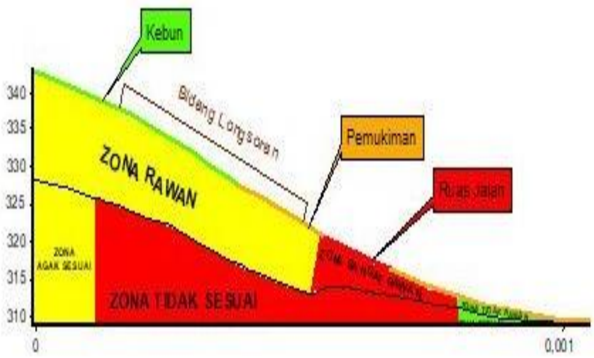

Fig. 7 Results of landslide cross section of Cikuya Village

Zoning map of landslide disaster prone areas through 3D visualization using Geo Camera application in Cikuya Village, Culamega District, Tasikmalaya District is created using scoring and weighting, namely overlaying the map of each variable or characteristic of landslide prone. Analyzed using Arcgis 10.5 mapping app, Surfer 10, Global Mapper 3D results can be viewed using Geo Camera app.

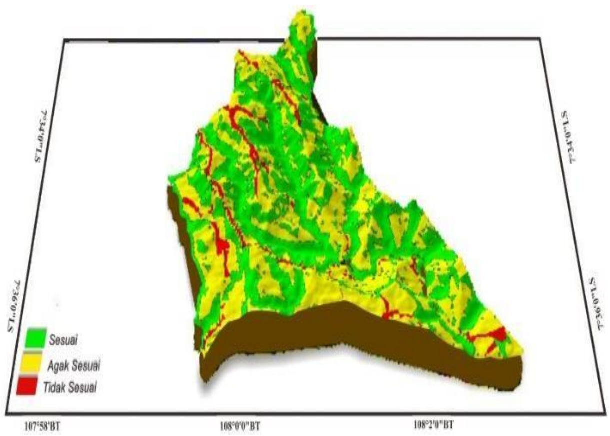

Fig. 8 Results of 3D map of landslide Prone zone

Fig. 9 View of landslide-prone 3D map and barcode scan on the Geo Camera App

Landslide disaster prone zoning map and land conformity analysis using Geo Camera application can be used in learning in schools as an interactive learning media in the form of 3D maps, can be used by teachers in teaching without using powerpoint viewer projectors or images because the form of maps displayed in 3-dimensional form only requires markers scanned using mobile phones by downloading the Geo Camera application.

4. CONCLUSION

Characteristics that cause landslides are high rainfall intensity ranging from 2,203 - 3,054 mm / year, Steep slopes range from 8° - 40°, geological conditions (types of rocks) are divided into two types, namely sedimentary rocks and volcanic rocks, podsolic yellow red soil types that are not good in water escape, as well as land use that is not in accordance with the conditions and carrying capacity of the region. The results of the analysis of assessment, weighting and overlay zoning of disaster-prone areas are divided into three "non-prone" hazardous landslide zones with an area of 7,597 hectares, a "prone" zone with an area of 1,972,147 hectares, and a "very vulnerable" landslide vulnerability zone with an area of 256,968 hectares. Further analysis is that land suitability is divided into three "appropriate" zones with an area of 1,057,391 Hectares, "somewhat appropriate" with an area of 1,080,373 Hectares, and "incompatible" with an area of 98,948 Hectares. Landsle-prone zoning in Cikuya Village, can be use as one of references by the government and the village community in craying out development and regional plan, forming evacuation teams and desaster response communities.

5. ACKNOWLEDGEMENTS

Special thanks given to the Community and stakeholders of Cikuya Village, Lecturers of Geography Education Unsil and Mr. Dr.Ir. Amien Widodo as a lecturer in Geological Disaster Mitigation Course, Permata Sakti program at ITS Campus that also directs and guides in completing this research.

References

[1] Arsyad, S. (2010) *Konservasi Tanah dan Air.* Bogor: IPB Press. Tersedia pada: http://repository.ipb.ac.id/handle/123456789/42667.

[2] bpbd Kabupaten Tasikmalaya (2020) *Draft Rencana Penanggulangan Bencana Kabupaten Tasikmalaya Tahun 2020-2024*. Tasikmalaya.

[3] DIBI BNPB (2019) "Jumlah Kejadian Bencana dan Kerugian Bencana di Indonesia."

[4] Eddy Prahasta (2009) *Sistem Informasi Geografi*. 1 ed. Bandung: Informatika.

[5] Hakim, Erwin Hilman, D. dan E. (2019) "Zonasi Rawan Bencana Longsor Sebagai Upaya Penatagunaan Lahandi Desa Bojongkapol Kecamatan Bojonggambir Kabupaten Tasikmalaya," in. Semarang: Proseding Seminar Nasional Geografi UMS X. Tersedia pada: https://hdl.handle.net/11617/11603.

[6] Harahap, S. dan Yanuarsyah, I. (2012) "Aplikasi Sistem Informasi Geografis (Sig) Untuk Zonasi Jalur Penangkapan Ikan Di Perairan Kalimantan Barat," *Jurnal Akuatika Indonesia*, 3(1), hal. (40-48). Tersedia pada: http://jurnal.unpad.ac.id/akuatika/article/view/477/569.

[7] Indarto, A. F. (2012) *Konsep Dasar Analisis Spasial*. 1 ed. Diedit oleh Sigit Suyantoro. Yogyakarta: Andi Offset.

[8] Sriyono (2017) *Geologi dan Geomorfologi Indonesia*. Yogyakarta: Ombak.

[9] Tribunnews.com (2017) "Bencana Longsor Terjang Tasikmalaya."